The 2009 IEEE/RSJ International Conference on
Intelligent Robots and Systems
October 11-15, 2009 St. Louis, USA

Three DOF Hybrid Mechanism for Humanoid Robotic Application: Modeling, Design and Realization

S. Alfayad, F.B. Ouezdou, F. Namoun, O. Bruneau, and P. Hénaff

Abstract— **This paper deals with a research work aimed to develop a new three degrees of freedom (DOF) mechanism for humanoid robots. The main idea is to build hybrid (3DOF) mechanism, which avoids the drawbacks of the serial and parallel mechanisms. The new solution has to merge the advantages of both classical (serial and parallel) structures in order to achieve optimal performances. The proposed mechanism can be used as a solution for several modules in humanoid robot. The hip mechanism is taken as an example to illustrate the contribution of this paper. To evaluate the performances of the system, simulation of this new mechanism is carried out with Adams software. Geometrical and Kinematic models are developed and included in the simulation tool. Based on biomechanical data, analysis of the new kinematic structure is carried out. The design of the proposed solution is then described. Finally the first prototype developed for the HYDROïD robot's hip is presented. This mechanism is a part of an International patent accepted at INPI- France.**

I. Introduction

The last years, several humanoid robots have been developed such as HRP2 [1], Asimo [2], H7 [3], Qrio [4], Wabian 2 [5], CB [6], with serial hip mechanism. Other humanoid robots have been built using parallel mechanism at the hip such as ROBIAN [7]. On one hand, serial hip structures are simple to be manufactured. Their geometrical properties, kinematics and dynamics models are easy to calculate and their control can be simpler than that of parallel mechanisms. However, hips made with serial mechanisms for each joint are often heavy. Furthermore each actuator has to support the weight of the following actuators of the hip of an open kinematic mechanism.

On the other hand, hips based on parallel mechanisms are robust and can produce important forces. They have also a high power to mass ratio. However, the different models used for control are not easy to establish, and make their control more difficult than for serial mechanisms.

Moreover, the workspace of the parallel mechanism hips is naturally smaller than that of the hips based on serial ones.

In another hand, to actuate humanoid robots, two technologies are used. Hydraulic technology is used to actuate for instance CB humanoid robot. Electric motors are used to actuate all the others robots listed above. Electric motors technology is a low cost one. However, it needs gearbox to adapt the power to the specific need. This induces a lot of intermediate mechanical parts and hence increases substantially the total weight of the system. Electric motors are well adapted for position control but much less effective for force control. Furthermore, they need including force sensors at the output, which makes difficult to perform compliant motions required to reproduce human walk efficiently.

Contrary to the electric motors, hydraulic actuation is a more expensive technology. However the technical advantages to generate compliant human-like motions naturally are obvious: high power to mass ratio, direct measures of the forces produced by the system and easy implementation of force control. Of course the drawback of this solution is linked to the central hydraulic group with its pipes passing through all the joints to arrive to the hip one.
Based on the pervious analysis, a novel hydraulic actuation technology was proposed by Alfayad et al [8]. This solution allows us to actuate the hip, with merging the advantages of both electric and classic hydraulic technologies.

The aim of this paper is to propose a new hybrid mechanism for humanoid robot hip, based on hydraulic technology, with the advantage of serial and parallel structures. The design of this new mechanism has to take into account some fundamental constraints related with humanoid robotic applications.

This paper is divided into five sections. In the second section, the fundamental constraints for the hips concerning the dimensions, the joint amplitudes and the required torques are given. In the third section the hip mechanism design taking into account these constraints is proposed. Furthermore its kinematic and geometrical properties are presented including singularities analysis. The fourth section is dedicated to the simulation results. The details of the real prototype and experimental results are given in the fifth section. At last, conclusion and further developments of this work are presented.

S. Alfayad is with the Laboratoire d'Ingénierie des Systèmes de Versailles (LISV), 10-12 Avenue de l'Europe, 78140 Vélizy, FRANCE (e-mail: sfayad@ hotmail.fr).

F. B. Ouezdou, with the Laboratoire d'Ingénierie des Systèmes de Versailles (LISV), 10-12 Avenue de l'Europe, 78140 Vélizy, FRANCE, (+33139254950; fax: +33139254985; e-mail: ouezdou@lisv.uvsq.fr).

F. Namoun is with the BIA Compagny, 8 rue de l'Hautil, 7800 Conflans-St- Honorine, FRANCE (e-mail: f.namoun@bia.fr).

O. Bruneau is with the Laboratoire d'Ingénierie des Systèmes de Versailles (LISV), 10-12 Avenue de l'Europe, 78140 Vélizy, FRANCE (e-mail: bruneau@ lisv.uvsq.fr).

P. Henaff is with the Laboratoire d'Ingénierie des Systèmes de Versailles (LISV), 10-12 Avenue de l'Europe, 78140 Vélizy, FRANCE (e-mail: henaff@ uvsq.lisv.fr).

II. FUNDAMENTAL CONSTRAINTS FOR THE HIP DESIGN

First of all, the design of the hip has to satisfy the geometrical and inertial distribution of the modified Hanavan model [9]. Secondly the joint motion ranges produced by a human during walking process have to be guaranteed.

Thirdly, a particular care with the power required for humanoid actuation, for the walk has to be taken. These three aspects are detailed in the following subsections.

A. Geometrical constraints

In order to achieve helpful interactive tasks with humans, a humanoid robot should have a full human size. The size of 1.6m and the weight of 50 Kg were chosen for our humanoid robot called HYDROïD, which is under development. These two parameters (height and weight) are used as inputs of the modified Hanavan model in order to produce dimensions, masses and centre of mass positions of the limbs of the complete humanoid robot. The results used for the design of the hip concern the lower part of the pelvis and the upper part of the leg. As a first approximation, the lower part of the pelvis has to be included in parallelepiped with the following dimensions: yaw $P_y = 183mm$, pitch $P_p = 230mm$, and roll $P_r = 160mm$.

The upper part of the leg has to be included in a truncated cone with the following dimensions: length $L_{leg} = 392mm$ mm, large radius $R_l = 74mm$ and small radius $R_s = 46mm$

Thus, the hip mechanism, which is a three dof joint, has to be included in the space defined by the lower part of the pelvis and the upper part of the leg (See Fig1).

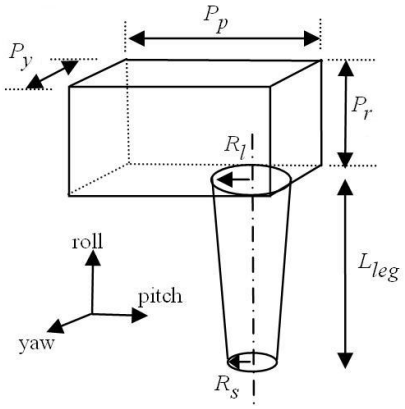

Fig.1 Allowed space for the hip mechanism

B. Motion range, speed and torque constraints:

Our aim is to design the hip of humanoid robot, which is able to walk with a speed equal to $1.2m/s$. In order to produce this speed, the required amplitudes of the joints of the hips have to be chosen. A large number of biomechanical studies have been done to analyse the motion of humans during the walk and mainly the joint motion amplitudes of the lower part of the humans [10], [11]. For a speed of $1.2m/s$, these studies show that the hip joint has $(-15^{\circ},+20^{\circ})$ around the pitch axis, $(-5^{\circ},+10^{\circ})$ around yaw axis and $(-5^{\circ},+5^{\circ})$ around roll axis.

These ranges have to be increased if other kinds of gaits such as climbing stairs are planed to be achieved with the humanoid robot. It is also well known that the pitch movement of human being has naturally an almost range of $(-90^{\circ},+90^{\circ})$.

Furthermore, it was observed that the maximum angular velocity for the hip around the pitch axis is 150 degrees per second for a walking speed equal to $1.2m/s$.

C. Needed torques

By studying dynamics [10], [11] and static equilibrium of a biped (height of 1.6m, weight of 50 kg), the mechanism hip torques were estimated to: 50 N.m around pitch axis, 35N.m around the yaw and the roll axes.

III. DESIGN OF THE HIP HYBRID MECHANISM

A. Analyzing existing hybrid hip mechanism

Let's start by shortly analyze the characteristics of the two others known hybrid hip mechanism used for biped robots. The first one is the three dof ROBIAN hip mechanism [7], which has 15 joints broken down into two closed loops (See Fig.2).

One of the advantages of this hybrid mechanism is that the pitch rotation RA is independent of the two others rotations (roll and yaw rotation). Indeed the pitch rotation requires the largest amplitude and closed chains are not really well adapted for this kind of large motion. The roll and yaw rotations which have comparable small amplitudes are produced by the two actuators LA1 and LA2. However, in the design of the ROBIAN hip, the pitch motion is produced after the yaw and rolls ones in the kinematic chain. The hip mechanism requires thus a lot of components and mechanical

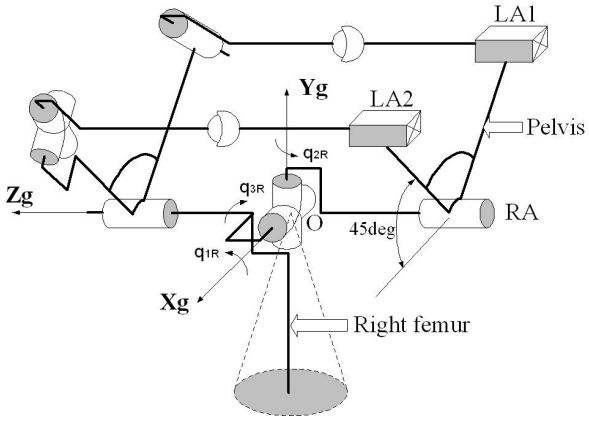

Fig.2 ROBIAN hip mechanism

parts.

This implies two major drawbacks: the first one is that the great number of mechanical parts induces large backlashes in

the hip. The second one is that it is very difficult to integrate all these components in the available space defined by the modified Hanavan model [9].

The other hybrid hip mechanism, developed for biped robot, has been proposed by Byung Rok et al [12]. Like ROBIAN hip, this mechanism has 15 joints split down into two closed chains (see Fig.3). One of the advantages of this mechanism is the position of its three actuators on the robot pelvis.

However, the independent joint chosen is the roll rotation joint, which presents small amplitude. Furthermore pitch rotation (large amplitude) and yaw rotation (small amplitude) are produced by the parallel mechanism. This choice requires large translation in the linear joints of the closed loops to produce pitch rotation. This implies two major drawbacks. Firstly, large backlashes in the hip can occur. Secondly, the large translations of the linear joints make it difficult to guarantee the geometrical constraints defined by the modified Hanavan model. Furthermore, this mechanism presents some risk of approaching singular positions.

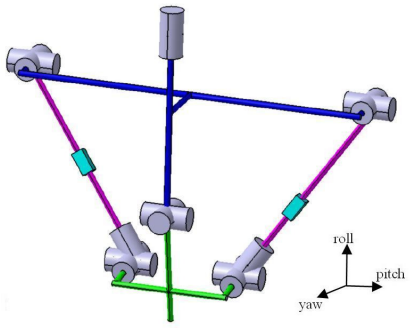

Fig.3 Byun Rok et al hip

B. *Proposed hybrid mechanism*

The proposed three dof hybrid mechanism, for HYDROïD humanoid robot has 17 joints broken down into two closed loops (see Fig.4 and Fig.5). Like ROBIAN hip, this new mechanism structure has the advantage that the pitch rotation is independent of the two others (yaw and roll). This allows us to produce motions around the pitch axis with large amplitude. The two linear actuators cooperate together to produce the angular motions around the yaw and the roll axes, which have small amplitudes. Since that the motion amplitudes around the yaw axis are greater than those around the roll axis, the hip design is made in such way that the two linear actuators work in the same direction for the yaw axis and in the opposite one for the roll axis movement.

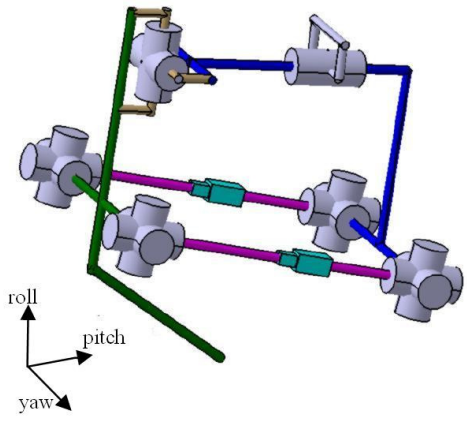

Fig.4 Proposed hybrid mechanism

As a result the small translation motions produced by the two linear actuators are sufficient to produce the rotation around the roll and yaw axis. Moreover contrary to ROBIAN hip, the pitch motion of HYDROïD hip is produced before the yaw and roll motions in the kinematic chain. This allows us to produce with the proposed mechanism larger motion amplitude for the pitch (flexion/extension) than the ROBIAN hip. The choices made for the new hip design lead to a compact mechanism with small number of mechanical components. The proposed mechanism satisfies also the constraints required by the modified Hanavan model.

Once the kinematic structure has been chosen based on the constraints listed above, the aim is to build a simulation tool of the new mechanism, which will enable us to carry out the earlier stage dimensioning process. To do so, it is necessary to achieve both geometrical and kinematic model of the proposed solution.

C. *Inverse Geometrical Model*

As the proposed solution has two closed chains, with 17 global dof, it is obvious that there is two internal random dof. Indeed, in each closed chain, this internal random dof concerns the rotation of the linear actuator around its axis. This internal random dof is due to the use of two spherical joint in each closed loop, which is recommended for symmetrical considerations that will be detailed later.

To develop the Inverse Geometrical Model (IGM), kinematic structure of the proposed mechanism is presented (see Fig.5) where several notations are adopted.

The j^{th} kinematic closed chain is presented by Ch_j for $j = 1,2$. The mechanism outputs are grouped in the vector $q = (q_s, q_v, q_f)$ given in Fig5. These angles are measured

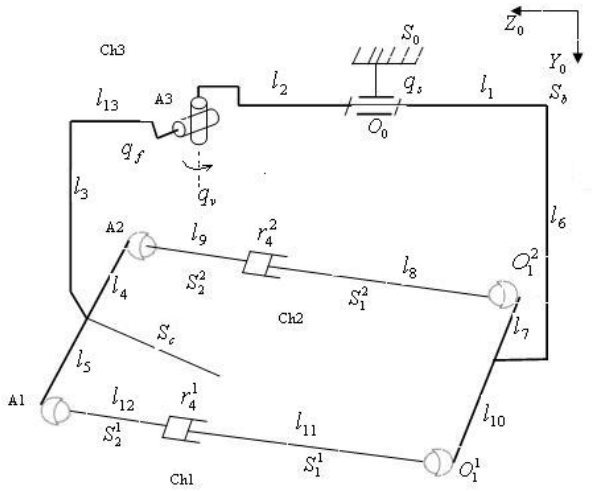

Fig.5 Kinematic model of the mechanism

thanks to the available sensors (see Mechanical Design pargarph). The mechanism inputs are the linear joint named r_4^j. Each spherical joint has been modeled by three perpendicular rotation joints (See Fig4). The angles $(\theta_1^1, \theta_2^1, \theta_3^1)$ are the three rotation constituting spherical joint located at O_1^1, while $(\theta_1^2, \theta_2^2, \theta_3^2)$ are those of the spherical joint positioned at O_1^2. In the same way, the spherical joint at A^1 is modeled by the three perpendicular angles $(\theta_5^1, \theta_6^1, \theta_7^1)$, while the last spherical joint located at A^2 is modeled by $(\theta_5^2, \theta_6^2, \theta_7^2)$. Finally l_k for $k = 1,2,...,13$ are the distances between joints centers as shown on Fig5.

The active variables are r_4^j, q_s while all the remaining joints are passive ones. All mathematical models will be established between those active variables and the outputs of the mechanism, defined privously by vector q.

The development of the IGM is based on the equivalent open mechanism method. This open chain obtained by breaking the random joint in A_j. By developing the two direct geometrical models of the left and right branch of open structure, the IGM can be established.

First we have to define the following basic variables:

$$f = \tan^{-1}(l_{13}/l_3), \qquad g_8 = \tan^{-1}(l_7/l_6) + \pi/2,$$
$$g_{12} = \pi/2 - \tan^{-1}(l_{10}/l_6), \qquad a = \sin(q_v), \qquad a_1 = \cos(q_v)$$

Then, the IGM of this first chain can be detailed as following:

$$\theta_1^1 = -\tan^{-1}\left(\frac{al_{14}\cos(f-q_f) - al_{15}\sin(g_8)}{l_{14}\sin(f-q_f) + al_{15}\cos(g_8) + a_1(l_1+l_2)}\right) \quad (1)$$

$$\theta_2^1 = -\tan^{-1}\left(\frac{\cos(\theta_1^1)(a_1 l_{14}\cos(f-q_f) - a_1 l_{15}\sin(g_8))}{l_{14}\sin(f-q_f) + al_{15}\cos(g_8) + a_1(l_1+l_2)}\right) \quad (2)$$

$$\theta_3^1 = \tan^{-1}\left(\sin(\theta_2^1)\tan(\theta_1^1) + \frac{\cos(\theta_2^1)(al_{14}\sin(f-q_f) + a_1 l_4 + l_{15}\cos(g_8))}{\cos(\theta_1^1)(a_1 l_{14}\sin(f-q_f) - l_4 a + l_2 + l_1)}\right) \quad (3)$$

Then the linear joint position r_4^1 can be calculated with the following expressions.

$$r_4^1 = \frac{a_1 l_{14}\sin(f-q_f) - l_4 a + l_2 + l_1}{\cos(\theta_2^1)\cos(\theta_3^1)} - l_8 - l_9 \quad (4)$$

In the same way, the IGM for the second chain can be achieved using the following relations:

$$\theta_1^2 = -\tan^{-1}\left(\frac{al_{14}\cos(f-q_f) - al_{16}\sin(g_{12})}{l_{14}\sin(f-q_f) + al_{16}\cos(g_{12}) + a_1(l_1+l_2)}\right) \quad (5)$$

$$\theta_2^2 = -\tan^{-1}\left(\frac{\cos(\theta_1^2)(a_1 l_{14}\cos(f-q_f) - a_1 l_{16}\sin(g_{12}))}{l_{14}\sin(f-q_f) + al_{16}\cos(g_{12}) + a_1(l_1+l_2)}\right) \quad (6)$$

$$\theta_3^2 = \tan^{-1}\left(\sin(\theta_2^2)\tan(\theta_1^2) + \frac{\cos(\theta_2^2)(al_{14}\sin(f-q_f) - a_1 l_5 + l_{16}\cos(g_{12}))}{\cos(\theta_1^2)(a_1 l_{14}\sin(f-q_f) + l_5 a + l_2 + l_1)}\right) \quad (7)$$

The second linear joint position r_4^2 is given by:

$$r_4^2 = \frac{a_1 l_{14}\sin(f-q_f) + l_5 a + l_2 + l_1}{\cos(\theta_2^2)\cos(\theta_3^2)} - l_{11} - l_{12} \quad (8)$$

Another advantage of achieving the (q_v, q_f) by the closed chain is due to the small range of movement produced by the spherical joints placed at O_1^j. This allows us the use of the IGM developed above in the control loop, as it will be detailed later.

D. Kinematic Models:

The aim of this paragraph is to establish the relation between the kinematic global variables named $\dot{X} = (\dot{\theta}_R, \dot{\theta}_Y, \dot{\theta}_P)$ and the input variables $\dot{r} = (\dot{r}_1^1, \dot{r}_1^2, \dot{q}_s)$. $\dot{\theta}_r$, $\dot{\theta}_y$ and $\dot{\theta}_p$ are the angular velocities in the roll, yaw and pitch directions respectively.

Using the kinematic composition formula, the kinematics of the j^{th} closed loop can be descibed as following:

$$Tc_{Sc/Sb} = Tc_{S1/Sb}^j + Tc_{S2/S1}^j + Tc_{Sc/S2}^j \quad (9)$$

Where $Tc_{sc/sb}$: is the kinematic wrench of the leg relative to the base of the parallel mechanism.

$Tc_{S1/Sb}^j$ is the kinematic wrench of the first body of the j^{th} linear actuator relative to the base of the parallel mechanism.

$Tc_{S2/S1}^j$ is the kinematic wrench of the j^{th} linear actuator.

$Tc_{Sc/S2}^j$ is the kinematic wrench of the leg relative to second body of the j^{th} linear actuator.

Based on the screw theory [13] Eq.9 can be written as:

$$Tc_{Sc/Sb} = \dot{\theta}_1^j \$_1^j + \dot{\theta}_2^j \$_2^j + \dot{\theta}_3^j \$_3^j + \dot{r}_4^j \$_4^j + \dot{\theta}_5^j \$_5^j + \dot{\theta}_6^j \$_6^j + \dot{\theta}_7^j \$_7^j$$

Where $\dot{\theta}_i^j$ is the derivative of the θ_i^j and $\$_k^j$: is the kinematic screw of the k^{th} joint in the j^{th} closed chain.

As r_4^j is the active variables in the closed chain, we can define the reciprocal screw of this variable, named $\$_1^{Rj}$, which satisfies:

$$\$_i^j \$_4^{Rj} = 0 \text{ for } i = 1,2,3,5,6,7 \qquad (10)$$

The frame R_1^j placed on O_1^j and parallel to R_0 is chosen to be the working reference frame for each closed chain. The j^{th} linear actuator projected in this frame can be written with its coordinates as:

$$A^j O_1^j = \begin{bmatrix} U_j & V_j & W_j \end{bmatrix}_{R_1^j}$$

Hence, given the reciprocal screw $\$_1^{R_j}$, the solution of the equations (10) can be established:

$$\$_4^{Rj} = \frac{1}{\sqrt{U_j^2 + V_j^2 + W_j^2}} \begin{bmatrix} U_j & V_j & W_j & 0 & 0 & 0 \end{bmatrix}$$

where $\sqrt{U_j^2 + V_j^2 + W_j^2} = \left\| A^j O_1^j \right\| \neq 0$

By multiplying Eq.(9) by this solution and by choosing A^j (See Fig.5) as working point for the j^{th} closed chain, the kinematic of the two closed chains can be presented as following:

$$\$_4^{R1} Tc_{Sp/S0}(A^1) = \dot{r}_4^1 \$_4^1 \$_4^{R1} \qquad (11)$$

$$\$_4^{R2} Tc_{Sp/S0}(A^2) = \dot{r}_4^2 \$_4^2 \$_4^{R2} \qquad (12)$$

The kinematic wrench of leg relative to the base s_b, projected on R_b can be written as:

$$Tc_{sp/R_1} = \dot{q}_v Z_v + \dot{q}_f Z_f = \begin{bmatrix} -\dot{q}_f C_{qv} & -\dot{q}_v & \dot{q}_f S_{qv} \end{bmatrix} \quad (13)$$

While the kinematic screw of the linear joint, projected on R_b can be presented as:

$$\$_{4/R_1^j}^j = \begin{bmatrix} -S_1 S_2 C_3 - C_1 S_3 & C_1 S_2 C_3 - S_1 S_3 & C_2 C_3 \end{bmatrix} \quad (14)$$

Where $C_i = \cos(\theta_i)$ and $S_i = \sin(\theta_i)$

Then, based on the advantage of this new hybrid structure, which makes the first rotation joint (q_s) independent of the two others joints (q_v, q_f) and by replacing Eq.13, Eq.14 in Eq.11 and Eq.12, the kinematic model can be established by the next equation named Eq 15:

$$\begin{bmatrix} 0 & -L_{13}U^1 - L_5 W^1 & -L_3 S_{qv} U^1 + L_{13} C_{qv} V^1 - L_5 S_{qv} V^1 - L_3 C_{qv} W^1 \\ 0 & -L_{13}U^2 + L_4 W^2 & -L_3 S_{qv} U^2 + L_{13} C_{qv} V^2 - L_5 S_{qv} V^2 - L_3 C_{qv} W^2 \\ 1 & 0 & 0 \end{bmatrix} \cdot \begin{bmatrix} \dot{q}_s \\ \dot{q}_v \\ \dot{q}_f \end{bmatrix} =$$

$$\begin{bmatrix} -U^1(S_1 S_2 C_3 + C_1 S_3) + V^1(C_1 S_2 C_3 - S_1 S_3) + W^1 C_2 C_3 & 0 & 0 \\ 0 & -U^2(S_1 S_2 C_3 + C_1 S_3) + V^2(C_1 S_2 C_3 - S_1 S_3) + W^2 C_2 C_3 & 0 \\ 0 & 0 & 1 \end{bmatrix} \begin{bmatrix} \dot{r}_4^1 \\ \dot{r}_4^2 \\ \dot{q}_s \end{bmatrix}$$

The last equation has the following classical matrix formulation:

$$A \cdot \dot{q} = B \cdot \dot{r}. \quad (16)$$

On the other hand, the global kinematic variable $\dot{X}$, defined previously, can be written as:

$$\dot{X} = \dot{q}_s Z_0 + \dot{q}_v Z_v + \dot{q}_f Z_f = \begin{bmatrix} \dot{q}_v S_{qs} - \dot{q}_f C_{qs} C_{qv} \\ -\dot{q}_v C_{qs} - \dot{q}_f S_{qs} C_{qv} \\ \dot{q}_s + \dot{q}_f S_{qv} \end{bmatrix}$$

$$\dot{X} = \begin{bmatrix} -C_{qs} C_{qv} & S_{qs} & 0 \\ -S_{qs} C_{qv} & -C_{qs} & 0 \\ S_{qv} & 0 & 1 \end{bmatrix} \begin{bmatrix} \dot{q}_f \\ \dot{q}_v \\ \dot{q}_s \end{bmatrix}$$

This can be reformulated as:

$$\dot{X} = D.\dot{q} \qquad (17)$$

Furthermore, the kinematic model of this new mechanism can be given by the following relation:

$$A \cdot D^{-1} \cdot \dot{X} = B \cdot \dot{r} \qquad (18)$$

E. Singularity analysis:

Once the kinematic model achieved, the first study to be done is singularity analysis, to ensure that the proposed mechanism works out of singularity position. Analyzing the D, A, B matrices leads to identify that the determinant of D matrix can be expressed as:

$$\det(D) = \cos(q_v) \quad (19)$$

Hence the first singularity position is $q_v = \pm\pi/2$.

On the other hand, the determinants of matrices A and B have been identified, with more complicated form than Eq.19. Analyzing those determinants, leads to a set of four singularities positions defined with the following conditions:

$q_v = \pm\pi/2$, $q_f \approx -\pi/3$, and $q_f \approx +2\pi/3$

As the roll and yaw rotations are the smallest rotation in the hip, then producing those rotations principally by the parallel mechanism, keep the q_v, q_f values far away from singularity position. This makes another advantage of the proposed mechanism.

IV. SIMULATION AND RESULTS

A. Virtual model

Based on the IGM, and kinematic models established above, virtual model of the hip has been built using Adams software (see Fig6). Real mass and inertial values of HYDROïD humanoid robot have been integrated in this simulation.

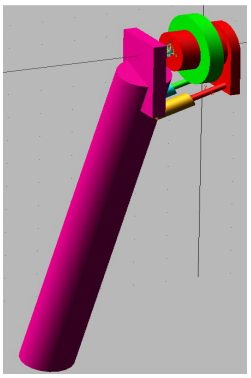

Fig.6 Hip virtual model

On the other hand, biomechanical data was obtained by analyzing natural human walk for speed $1.2m/s$. Using motion capture system [14] and inverse dynamic models, effort applied by the knee on the leg during this walk, has been calculated. These effort components were integrated on the virtual model to simulate the natural walk environment for the hip.

A PID control loop based on the inverse geometrical and kinematic models has been built (See Fig.7). To let the proposed hip mechanism following the desired motion, the inputs of this control loop are the desired hip angles $X_d = (\theta_R^d, \theta_Y^d, \theta_P^d)$.

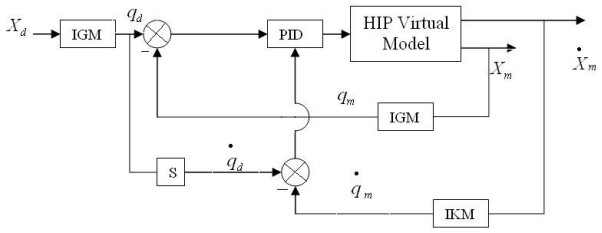

Fig.7 Control loop

A. *Simulation results*

i) Variables lengths and active joint ranges: Based on the fact that, for constant pressure value, increasing l_3, l_4, l_5, l_6 (see Fig.5) will increase the produced torque at the hip joint, those parameters have been chosen to be the biggest values in the available volume. On the other hand, once the nominal pressure is chosen, active surface of the pistons needed to guarantee the nominal torque at the hip joint is calculated. On the other hand, using the IGM, the maximum values of the linear actuators needed to reach all the useful workspace are determined by simulation. This leads to $r_4^j \approx 50mm$.

Once the virtual model has been built, the first results are to analyze the linear active joint variation during the desired walk. These variations given by Fig.8 are not symmetric for the initial positions of the linear actuators. This will induce changing the variables l_8, l_9, l_{11}, l_{12} (see Fig.5) in such away to bring these variations to be symmetric.

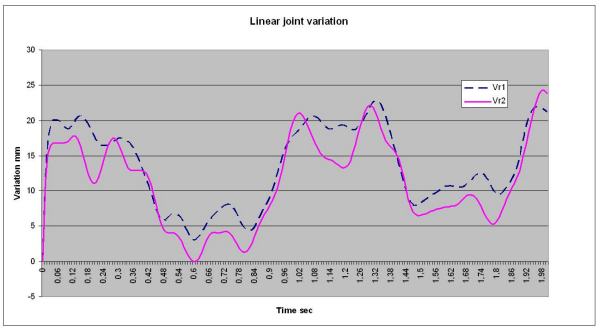

Fig8 Linear joint variation

ii) Joint positions, efforts and needed torques: Fig.9 shows the hip yaw angle achieved by the PID controller during the simulation of walking gait. The desired and the measured (with Adams) values are both plotted on Fig.9.

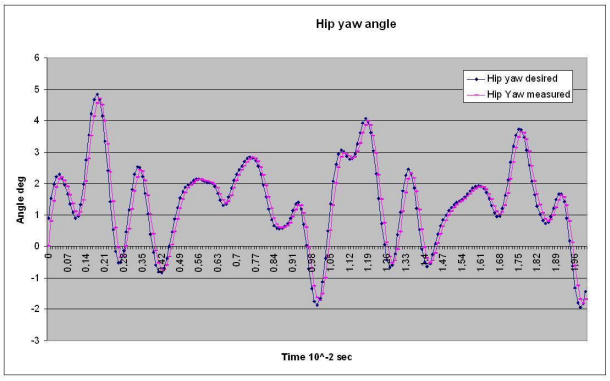

Fig9 hip yaw angle

Another aspect, which is important in early stage dimensioning process, concerns the forces in the joints. These forces fix the geometrical and the material properties that should be chosen for the final prototype. Fig. 10 gives the magnitude of the force at the level of the spherical joint located at O_1^1 and this at O_1^2 as an example of this kind of joint force unknown

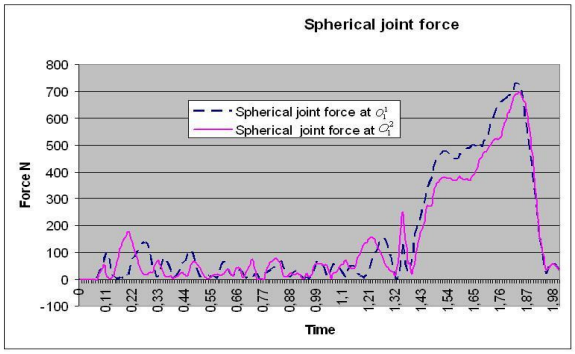

Fig10 Spherical joints force

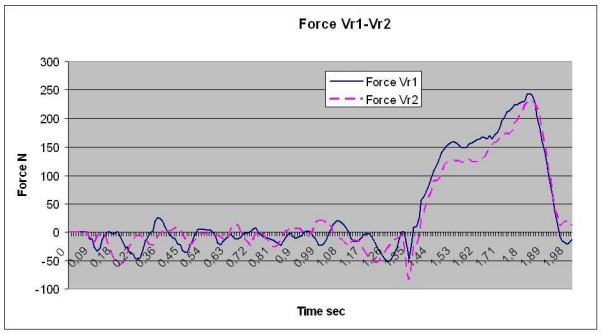

Fig11.Linear actuators forces

Finally, it is important to determine the total force needed for the active joints. This will fix the nominal pressure to be used for the pistons. Fig.11 gives the required forces for linear actuautors $\{r_4^1, r_4^2\}$ during walking cycle.

B. Realized prototype

This hip was designed to support continuous maximal pressure of $100bar$, while the nominal pressure to produce needed torque is $30bar$ which give us a save side more then three times in terms of output produced torque. Fig. 12 presents the realized prototype.

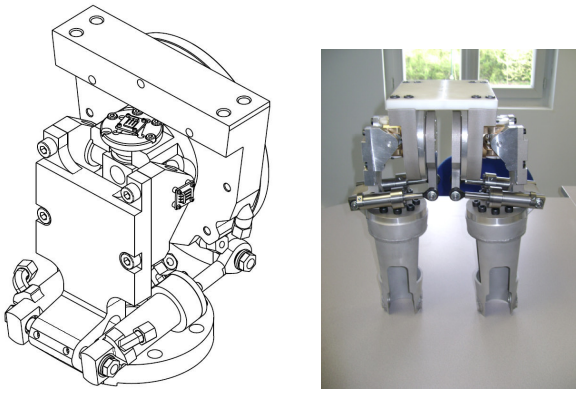

Fig.12 3D CAD and a picture of the realized prototype

V. CONCLUSION

In this paper, a novel hybrid mechanism was presented, for humanoid robotic applications. The advantages of the proposed mechanism were detailed in comparison with serial and parallel usual hips. Global biomechanical constraints were listed and respected. Importance care was taken to fit within the available volume. Geometrical and kinematic studies were achieved to analyze the mechanism properties. Singularity study has been realized to show another advantage of this mechanism.

A simulation tool based on Adams was developed, in which biomechanical data, as mass, inertia, external effort applied on the hip during walk have been integrated. Control loop based on the geometrical and kinematic model has been used. Results of position control, linear actuator force, and spherical joint force for the three hip angles were shown. The proposed solution is a part an international patent registered at INPI- France.

Finally, preliminary experimental video is included to show the motions of the realized prototype designed for HYDROID robot.

The further work concerns the control of this mechanism with the hydraulic energy converter during the achievements of HYDROïD first experiments.

KNOWLEDGMENT

This work was carried out in the frame of the ANR-Blanc research project called PHEMA. It was also supported by BIA Company. We thank very strongly both supports.

REFERENCES

[1] K. Kaneko, F. Kanehiro, S. Kajita, H. Hirukawa, T. Kawasaki, M; Hirata, K. Akachi, and T. Isozumi, «Humanoid robot HRP-2,» in Proc. IEEE Int. Conf. Rob. Aut. (ICRA), NewOrleans, USA, 2004, pp. 1083-1090.

[2] http://asimo.honda.com/

[3] K. Nishiwaki, S. Kagami, J. Kuffner, M. Inaba, and H. Inoue, «Humanoid «JSK-H7»: Research platform for autonomous behavior and whole body motion,» in Proc. Int. Workshop Humanoid and human friendly robotics (IARP), Tsukuba, Japan, 2002, pp. 2-9.

[4] http://www.kitt.net/blog/gadget/2005/01/sony-qiro-biped-robot.html

[5] Yu Ogura, Hiroyuki Aikawa, Kazushi, Shimomura, Hideki Kondo, and Akitoshi Morishima, Hun-ok Lim Atsuo Takanishi, "Development of a New Humanoid Robot WABIAN-2", Proc. of IEEE ICRA 2006, pp 76-81,Orlando, Florida

[6] G. Cheng, S-H. Hyon, J. Morimoto, A. Ude, J. G. Hale, G. Colvin, W. Scroggin, and S. Jacobsen. (2007). CB: A humanoid research platform for exploring neuroscience. Journal of Advance Robotics, 21, 10, 1097-1114.

[7] A. Konno, R. Sellaouti, F. B. Amar and F. B. Ouezdou, «Design and Development of the Biped Prototype ROBIAN». Dans «IEEE - (ICRA)», p. 1384–1389, 11-15 May 2002. Washington, D.C., U.S.A. URL

[8] S. Alfayad, F.B. Ouezdou, F.Namoun, G. Cheng, « Lightweight High Performance Integrated Actuator for Humanoid Robotic Applications: Modeling, Design & Realization» in Proc. IEEE Int. Conf. Rob. Aut. (ICRA), Kobe, Japan, 2009.

[9] F. Gravez, O. Bruneau, F.B. Ouezdou, "Analytical and automatic modeling of digital humanoids", (IJHR), World Scientific, Vol.2, N°3, pp 337-359, september 2005.

[10] Sanderson D.J.1; Martin P.E. "Lower extremity kinematic and kinetic adaptations in unilateral below-knee amputees during walking", Gait and Posture, Volume 6, Number 2, October 1997 , pp. 126-136(11)

[11] Rietdyk Shirley. "Lower Anticipatory locomotor adjustments of the trail limb during surface accommodation", Gait and Posture, Volume 23, Issue 3, April 2006,Pages 268-272

[12] So Byung, Yi.Byung, K.Wheekuk, S.Rok, P.Jongil, K.Youn Soo. "Design of a Redundantly Actuated Leg Mechanism",. (ICRA),, Taipei, Taiwan, September 14-19 2003

[13] Duffy, J. "The Fallacy of Modern Hybrid Control Theory that is Based on Orthogonal Complements of Twist and Wrench Spaces", Journal of Robotic Systems, vol. 7(2): , 1990, pp. 139-144.